BUCKLING OF WING SPARS UNDER COMBINED LOADING

David Kennedy*, Dharmesh C. Patel*, Carol A. Featherston*
*Cardiff School of Engineering, Cardiff University, Queen's Buildings, The Parade,
Cardiff CF24 3AA, U.K.

Keywords: *spars, critical buckling, compression, bending, shear*

Abstract

Design rules for the prediction of critical buckling stresses in aircraft wing spars are extended to cover loading cases which include uniform transverse compression. Curve fitting for pure loading cases enables numerical predictions to be made of the stiffener dimensions required to provide effective simple support to the skin, and of the critical buckling stress for panels of arbitrary dimensions. A proposed extension of the method to combined loading cases is outlined.

1 Introduction

Spars in aircraft wing boxes are long integrally machined channel sections consisting of panels separated by vertical stiffeners, as shown in Fig. 1(a). The purpose of the spar is to provide one of the main load paths for vertical shear loading. Therefore critical buckling is a major consideration in the design of spar panels, either as a primary design criterion or to indicate the onset of postbuckling.

For the simplified infinitely long spar models of Fig. 1(b), theory has long been available [1] to predict the critical shear buckling stress for a range of skin and stiffener dimensions. Corresponding results for longitudinal compressive loading and in-plane bending have recently been presented [2].
Combined loading cases are often handled using empirical design rules, or "interaction equations", representing (usually quadratic) interaction surfaces relating two (or more) of the component stresses at critical buckling [3-6]. A previous study [2] verified the interaction equation
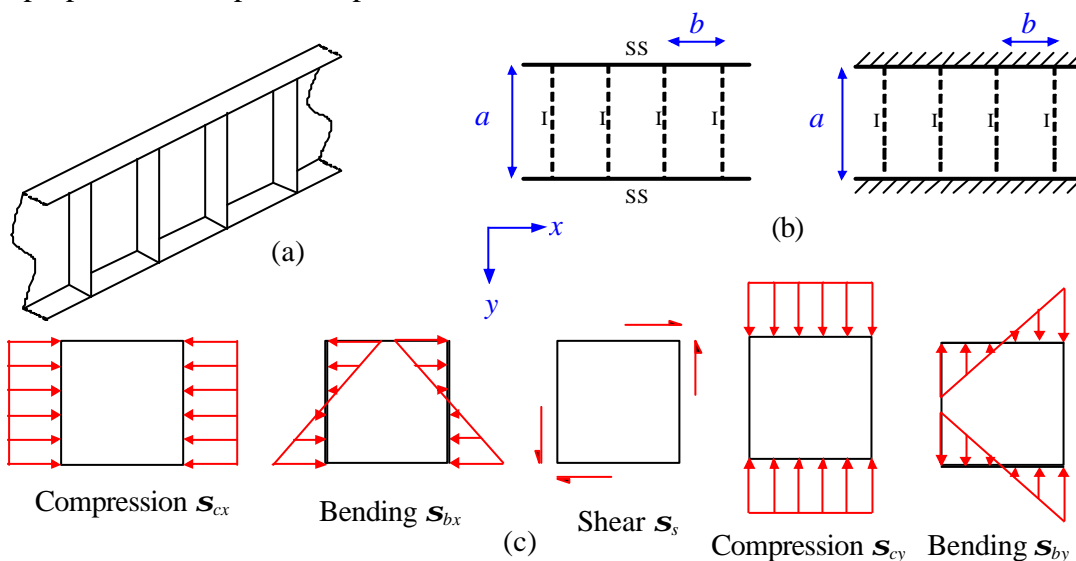
Fig. 1 (a) Diagrammatic representation of a wing spar. (b) Simplified model showing simply supported and clamped edge conditions on the longitudinal edges. (c) Loading cases.

$$R_{cx} + R_{bx}^2 + R_s^2 = 1 \qquad (1)$$

for a simply supported isotropic plate with a wide range of aspect ratios, and hence for spar panels, such as those of Fig.1(a), whose stiffeners effectively provide simple support to the skin. Here

$$\left. \begin{array}{l} R_{cx} = \boldsymbol{s}_{cx} \big/ \overline{\boldsymbol{s}}_{cx} \\ R_{bx} = \boldsymbol{s}_{bx} \big/ \overline{\boldsymbol{s}}_{bx} \\ R_s = \boldsymbol{s}_s \big/ \overline{\boldsymbol{s}}_s \end{array} \right\} \qquad (2)$$

where $\boldsymbol{s}_{cx}$, $\boldsymbol{s}_{bx}$ and $\boldsymbol{s}_s$ are the longitudinal compressive, bending and shear stresses at critical buckling in a combined loading case, as shown in Fig. 1(c), while $\overline{\boldsymbol{s}}_{cx}$, $\overline{\boldsymbol{s}}_{bx}$ and $\overline{\boldsymbol{s}}_s$ are the critical buckling stresses for the respective single loading cases.

This paper extends the analysis to spar panels loaded in uniform transverse compression $\boldsymbol{s}_{cy}$. After studying the effect of stiffener size on the critical buckling stress $\overline{\boldsymbol{s}}_{cy}$, critical buckling stresses are determined for simply supported plates under combined loading cases which include transverse compression, providing a generalisation of Eq. (1). Finally, for the single loading cases, an attempt is made to quantify the stiffener sizes needed to provide effective simple support and the reduction in critical buckling stress when smaller stiffeners are used. This enables reliable critical buckling predictions to be made using simple calculations based on the spar geometry.

The results in this paper were obtained using the software VICONOPT [7], which covers prismatic assemblies of rectangular plates, each of which can carry any combination of the in-plane stresses $\boldsymbol{s}_{cx}$, $\boldsymbol{s}_s$ and $\boldsymbol{s}_{cy}$ of Fig. 1(c), which are assumed to be invariant in the longitudinal (x) direction. A longitudinal bending stress $\boldsymbol{s}_{bx}$ is modelled by dividing the plate into n_b longitudinal strips carrying longitudinal compressive stresses $\boldsymbol{s}_{bx}\big[\big((2i-1)/n_b\big)-1\big]$, $i=1,2,\ldots n_b$. Accuracy was guaranteed by using $n_b = 70$, although in

most cases adequate results are obtained with $n_b = 20$. Transverse bending stresses $\boldsymbol{s}_{by}$ were not considered.

The analysis is based on the exact solution of the governing differential equations of the plates, yielding exact stiffness matrices whose elements are transcendental functions of the load factor. In the simplest form of the analysis [8], the buckling mode is assumed to vary sinusoidally in the x direction with half-wavelength l. Shear loaded panels are more accurately modelled by combining such responses [9] for an infinitely long panel whose end supports repeat at intervals of the panel length l. This approach, which has been adopted in the present paper, also permits the stiffeners to be modelled as transverse beam supports with no torsional stiffness.

2 Pure Loading Cases

2.1 Review of Previous Results

Critical buckling results for spar panels have previously been obtained [2] for the three load cases of uniform longitudinal compression $\boldsymbol{s}_{cx}$, longitudinal bending $\boldsymbol{s}_{bx}$ and in-plane shear $\boldsymbol{s}_s$, for the two longitudinal edge support conditions shown in Fig. 1(b). For each case, the VICONOPT results were verified by comparison with published results [1] or by finite element analysis.

Design curves for isotropic spar panels are obtained as non-dimensional plots of the critical buckling parameter K against the stiffener parameter $\boldsymbol{m}$, defined by

$$\left. \begin{array}{l} K = \overline{\boldsymbol{s}}_{\bullet} b^2 \big/ Et^2 \\ \boldsymbol{m} = \sqrt{\dfrac{t_s b_s^3 b}{3a^2 t^3}} \end{array} \right\} \qquad (3)$$

where $\overline{\boldsymbol{s}}_{\bullet}$ ($\bullet = cx, bx, s$) is the critical buckling stress, E is Young's modulus, the panel has width a and stiffener spacing b, while the stiffeners are modelled as blades with depth b_s
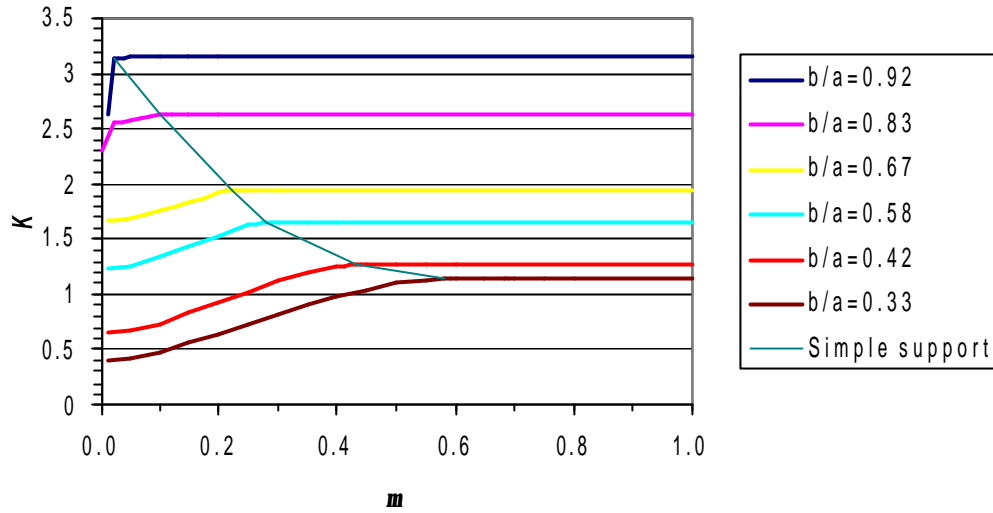
Fig. 2. Critical buckling parameter K against stiffener parameter m for a spar panel with simply supported longitudinal edges, loaded in longitudinal compression. The faint line connects the transition points $m = m_s$, beyond which the stiffeners effectively provide simple support.

and thickness t_s. The torsional stiffness of the stiffeners is neglected. Typical plots for longitudinal compression and shear loading are shown in Figs. 2 and 3, respectively, for a range of aspect ratios b/a. Each plot shows a transition between the limiting cases of an infinitely long unstiffened plate (at $m = 0$) and a panel with transverse simple supports repeating at intervals of b. During this transition there are changes in the buckling mode shape. In the

case of longitudinal compression, the points $m = m_s$ at which the stiffeners effectively provide simple support are well defined (and plotted in Fig. 2), denoting an abrupt change in mode shape. If $m > m_s$, K matches analytical predictions [10] and shows no further increase. In contrast, there is a gradual transition of the shear buckling modes associated with Fig. 3 so that m_s is less well defined and the limiting value of K must be found asymptotically.
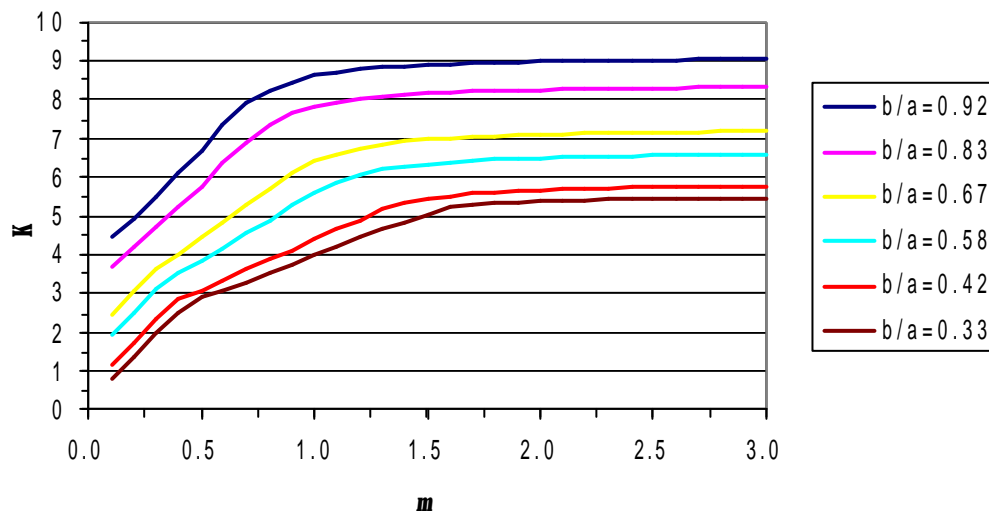
Fig. 3 Critical buckling parameter K against stiffener parameter m for a spar panel with simply supported longitudinal edges, loaded in shear.
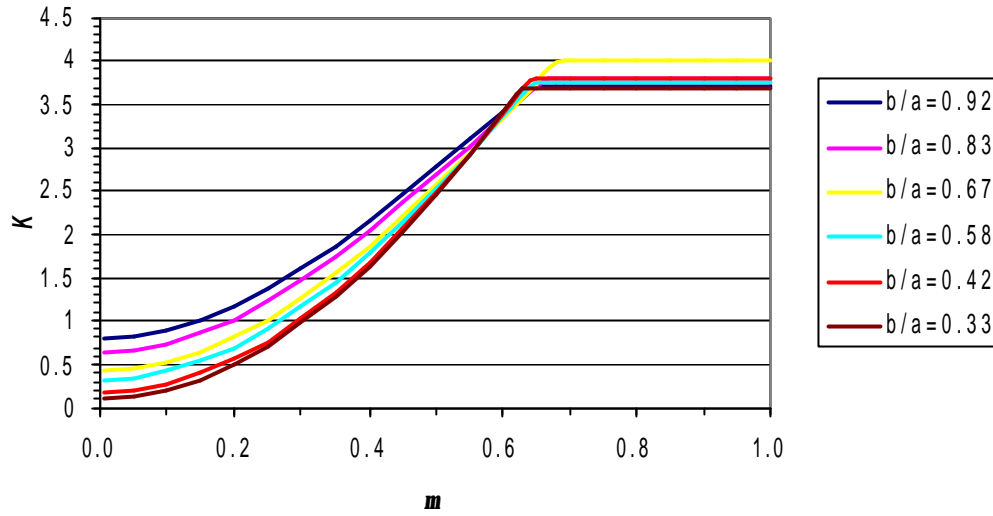
Fig. 4. Critical buckling parameter K against stiffener parameter m for a spar panel with simply supported longitudinal edges, loaded in transverse compression.

2.2 Uniform Transverse Compression

Using VICONOPT analysis, critical buckling stresses have been found for spar panels loaded in uniform transverse compression s_{cy}, for a range of aspect ratios b/a and stiffener sizes. The results, represented by the parameters K and m of Eq. (3) with $\overline{s}_{\bullet} = \overline{s}_{cy}$, are shown in Fig. 4.

When $m = 0$, the critical buckling stress matches that of an infinitely long unstiffened plate of width a under uniform transverse compression, which is equivalent to column buckling for a plate of length a with free longitudinal edges under uniform longitudinal compression.

For large values of m, the stiffeners effectively provide simple support and K matches analytical predictions for a simply supported plate [10]. This condition is reached at a well defined point $m = m_s$, which (unlike the loading cases of Figs. 2 and 3) is relatively insensitive to the panel aspect ratio. The dramatic change in slope at $m = m_s$ for each of the plots of Fig. 4 indicates a change in the shape of the critical buckling mode.

Non-uniform transverse loading cannot be modelled easily by VICONOPT and so the transverse bending case s_{by} has not been considered in the present work. However for $m > m_s$, some analogies with the longitudinal bending case s_{bx} can be drawn by considering a simply supported plate with the x and y axes interchanged.

3 Combined Loading Cases

3.1 Review of Previous Results

Figures 2-4 show that a spar panel with vertical stiffeners of stiffness $m \geq m_s$ can be adequately modelled by a simply supported plate of width a and length b, representing the portion of skin between adjacent stiffeners. Such plates of varying aspect ratio b/a have previously been analysed [2] for combined loading cases including uniform longitudinal compression s_{cx}, longitudinal bending s_{bx} and in-plane shear s_s. Typical interaction curves are shown in Fig. 5. The results show that, except for some extreme aspect ratios, the predictions given by Eq. (1) are accurate to within a few percent and are almost always conservative, i.e. underestimating the stresses at critical buckling.
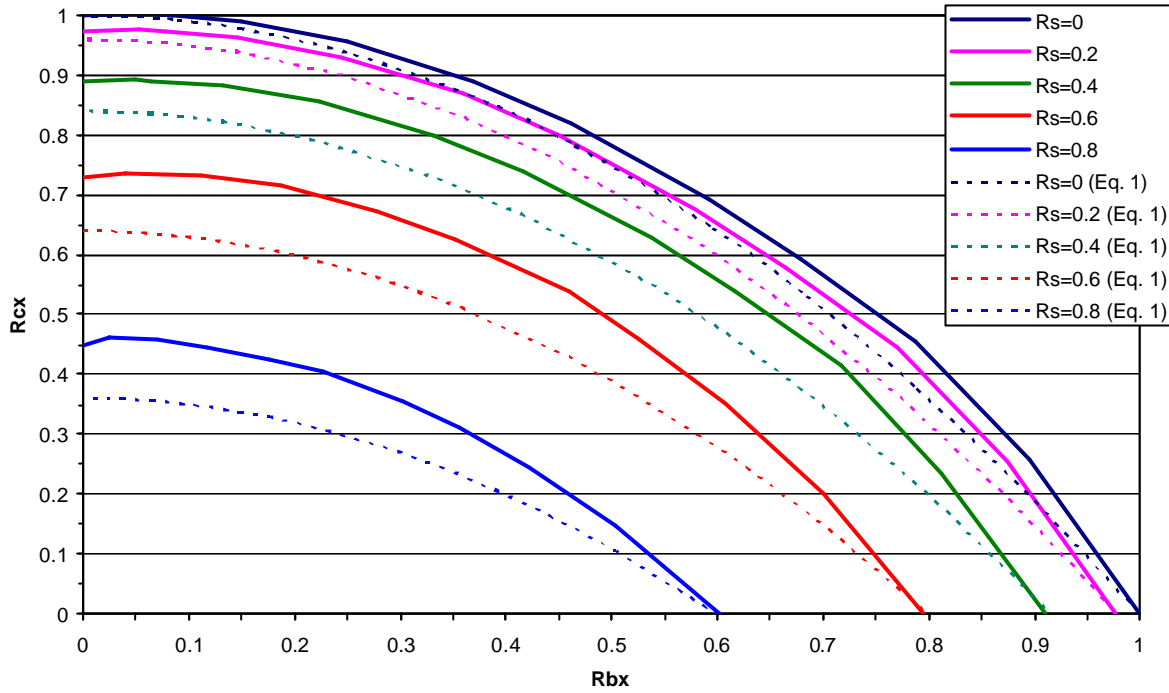
Fig. 5. Critical buckling criteria for a simply supported plate with $b/a=1$, loaded in longitudinal compression $\mathbf{s}_{cx}$, longitudinal bending $\mathbf{s}_{bx}$ and in-plane shear $\mathbf{s}_s$. Each solid curve shows VICONOPT results for the compression-bending interaction at a particular value of the shear stress parameter R_s, while the corresponding dashed curve shows the criteria predicted by Eq. (1).

3.2 Inclusion of Transverse Compression

The critical buckling criterion for a simply supported plate of width a and length b, loaded in uniform longitudinal and transverse compression, has been derived [10] as

$$m^2 \mathbf{s}_{cx} + n^2 \frac{b^2}{a^2} \mathbf{s}_{cy} \tag{4}$$

$$= \frac{\mathbf{p}^2 E t^2}{12(1-\mathbf{n}^2)b^2}\left(m^2 + n^2 \frac{b^2}{a^2}\right)^2$$

where the buckling mode has m and n half-waves in the longitudinal and transverse directions, respectively, and $\mathbf{n}$ is Poisson's ratio. The linear relationship of Eq. (4) means that the interaction diagram between $\mathbf{s}_{cx}$ and $\mathbf{s}_{cy}$ is a series of intersecting straight lines. For example, if $b/a=1$ and $\mathbf{s}_{cx}$ and $\mathbf{s}_{cy}$ are both compressive (i.e. positive), then critical buckling always occurs with $m=n=1$. However the critical buckling mode can have a higher value of m or n if one of the stresses is

tensile (i.e. negative). Results obtained using VICONOPT match this analytical prediction.

It is therefore suggested that, for combined loading cases including transverse compression, the ratio

$$R_{cy} = \mathbf{s}_{cy} / \overline{\mathbf{s}}_{cy} \tag{5}$$

plays a similar role to that of R_{cx} in the interaction equation. This has been confirmed by studies of the interaction between transverse compression and shear loading for aspect ratios in the range $0.25 \leq b/a \leq 1$, giving the revised, usually conservative, critical buckling criterion

$$R_{cx} + R_{bx}^2 + R_s^2 + R_{cy} = 1 \tag{6}$$

More evidence is needed to confirm that the critical buckling criterion can be further extended to give

$$R_{cx} + R_{bx}^2 + R_s^2 + R_{cy} + R_{bx}^2 = 1 \tag{7}$$

where

$$R_{by} = \mathbf{s}_{by} / \overline{\mathbf{s}}_{by} \tag{8}$$

and $\overline{s}_{by}$ is the critical buckling stress under transverse bending.

4. Prediction of Critical Buckling Stress

4.1 Parameter Estimation

The effects of stiffener size on the critical buckling stress of a wing spar have been shown in Figs. 2-4 for pure loading cases. This section illustrates, for a panel of arbitrary aspect ratio, the estimation of the stiffness parameter m_s beyond which the stiffeners effectively provide simple support. Estimates are also given of the critical buckling parameter K when $m < m_s$. The analysis is presented for panels loaded in uniform longitudinal compression, using the results of Fig. 2, and can readily be applied to other pure loading cases.

The faint line in Fig. 2 connects the points where $m = m_s$ for different aspect ratios b/a. Least squares fitting of a cubic polynomial to this data gives the relationship

$$m_s = 1.5676 - 4.3287(b/a) \qquad (9)$$
$$+ 4.7511(b/a)^2 - 1.9840(b/a)^3$$

with correlation coefficient $r^2 = 0.9972$. The asymptote $m_s = 0.02$ is assumed when $b/a > 1$. Attempts were made to fit polynomial curves to the K against m curves of Fig. 2, but this proved unreliable due to the changes in gradient at $m = m_s$.

In general a better fit was obtained by using the Boltzmann curve

$$K = \frac{K_1 e^{(m_0/a)} + K_2 e^{(m/a)}}{e^{(m_0/a)} + e^{(m/a)}} \qquad (10)$$

illustrated in Fig. 6. Here K varies monotonically between a lower limit K_1 and an upper limit K_2, taking the value $0.5(K_1 + K_2)$ at $m = m_0$. The parameter a controls the rate of increase from K_1 to K_2. Least squares curve fitting gave the parameters
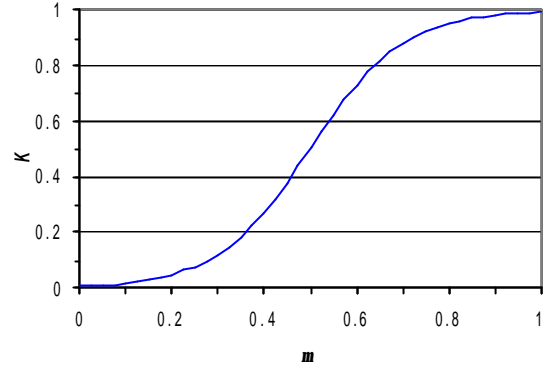
Fig. 6. Boltzmann curve of Eq. (10), with K_1=0, K_2=1, m_0=0.5 and a=0.1

$$\left.\begin{matrix} K_1 = 0.1510 & K_2 = 1.0498 \\ m_0 = 0.3156 & a = 0.1389 \end{matrix}\right\} \qquad (11)$$

with correlation coefficient $r^2 = 0.9978$ for the aspect ratio $b/a = 0.25$ (which is not shown in Fig. 2). As expected, the fitted values of K_1 and K_2 are close to the values of K at $m = 0$ and $m = m_s$, respectively, and $m_0 \cong 0.5 m_s$. However considering only the points in the range $m < m_s$ gave an even better fit

$$\left.\begin{matrix} K_1 = 0.0529 & K_2 = 1.1208 \\ m_0 = 0.3061 & a = 0.1810 \end{matrix}\right\} \qquad (12)$$

with correlation coefficient $r^2 = 0.9995$. Although this refinement tends to overestimate the upper limit of K, it has been adopted hereafter in a hybrid form which predicts K from the Boltzmann curve when $m < m_s$ and from analytical results for simply supported plates [10] when $m \geq m_s$. The hybrid approach correctly predicts the changes in gradient in the K against m curves at $m = m_s$.

Repeating the Boltzmann curve fitting for different aspect ratios b/a gives families of values for the parameters K_1, K_2, m_0 and a. Next, these parameters are each fitted by cubic polynomials in b/a, with correlation coefficient $r^2 > 0.999$ in each case, to give

$$K_1 = -0.5694 + 2.3092(b/a)$$
$$+ 0.2874(b/a)^2 + 1.7450(b/a)^3$$

$$K_2 = 1.0115 + 0.0563(b/a)$$
$$+ 1.1838(b/a)^2 + 1.3317(b/a)^3$$

$$m_0 = 0.5317 - 1.2319(b/a)$$
$$+ 1.5107(b/a)^2 - 0.8392(b/a)^3$$

$$a = 0.5161 - 1.9973(b/a)$$
$$+ 3.0072(b/a)^2 - 1.5956(b/a)^3$$

(13)

4.2 Numerical Predictions

Using the parameters established in section 4.1, it is now possible to predict the critical buckling parameter K for wing spars of arbitrary skin and stiffener dimensions. A simple Visual Basic computer program has been written to the specification of Table 1.

Fig. 7 gives some illustrative results for a spar panel loaded in uniform longitudinal compression, for three different aspect ratios b/a. The results show that the values of K predicted by the program are conservative and accurate to within a few percent.

Table 1. Prediction of critical buckling parameter K for a pure loading case.

Step	Task
1	Input skin dimensions a, b, t and stiffener dimensions b_s, t_s.
2	Calculate m using Eq. (3).
3	Calculate m_t using Eq. (9).
4(a)	If $m < m_t$, calculate K using Boltzmann curve of Eq. (10) with parameters K_1, K_2, m_0, a given by Eq. (13).
4(b)	If $m \geq m_t$, calculate K using analytical results for a simply supported plate [10].

In order to extend the predictions to combined loading cases, it is convenient to define a stress vector

$$\mathbf{s} = \{s_{cx}, s_{bx}, s_s, s_{cy}, s_{by}\} \qquad (14)$$

It is required to find the critical buckling factor F, such that buckling occurs when

$$\mathbf{s} = F\{s_{cx0}, s_{bx0}, s_{s0}, s_{cy0}, s_{by0}\} \qquad (15)$$

where $s_{\bullet 0}$ ($\bullet = cx, bx, s, cy, by$) represents a set of base stress values. Steps 3 and 4 of Table 1 must be carried out for each component of stress $s_\bullet$, giving a family of parameters $K_\bullet$, from which the critical buckling stresses $\bar{s}_\bullet$ for each of the pure loading cases can be calculated
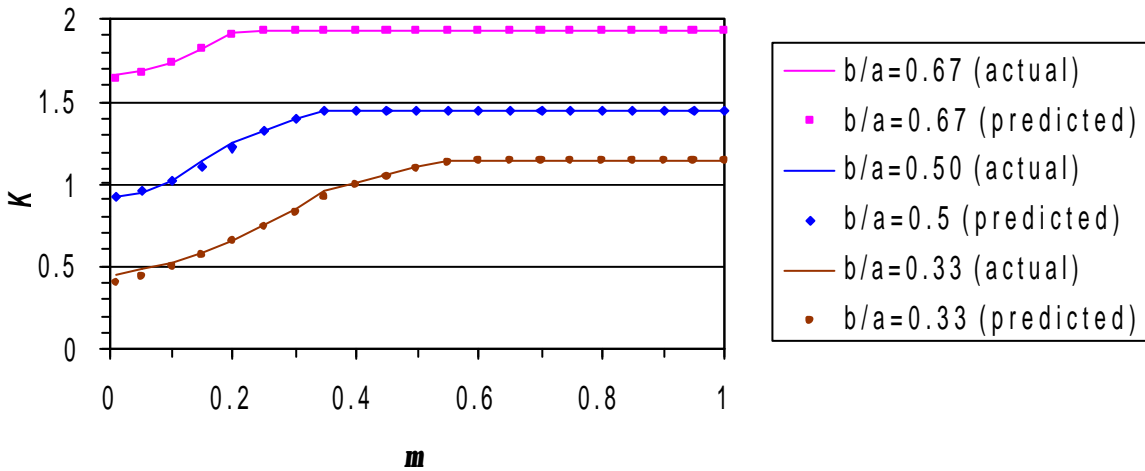
Fig. 7. Actual and predicted critical buckling parameters K for a spar panel with simply supported longitudinal edges, loaded in longitudinal compression.

using Eq. (3). Then, using base values of the stress ratios

$$R_{\bullet 0} = s_{\bullet 0}/\overline{s}_{\bullet} \qquad (16)$$

in Eqs. (7) and (15), the critical buckling criterion F is obtained from the equation

$$F^2\left(R_{bx0}^2 + R_{s0}^2 + R_{bx0}^2\right) \qquad (17)$$
$$+ F\left(R_{cx0} + R_{cy0}\right) - 1 = 0$$

which always has one positive root.

5 Concluding Remarks

Parametric studies have previously been carried out, using an exact strip method, on the effect of stiffener dimensions on the critical buckling of aircraft wing spars subjected separately to longitudinal compression, in-plane shear and bending stresses. In each case, increasing the stiffener second moment of area increases the critical buckling stress from its theoretical value for an unstiffened plate of infinite length to a higher value matching that of an unstiffened plate with simply supported ends and length equal to the stiffener spacing. Results for combined loading cases can be predicted using a simple interaction equation.

The present work has extended the analysis to wing spars loaded in pure transverse compression, and has also established interaction relationships for combined load cases which include transverse compression.

Numerical predictions have been made of the stiffener dimensions required to provide effective simple support to the skin, for a range of panel aspect ratios. For pure loading cases, the relationship between critical buckling stress and stiffener dimensions has been fitted to a non-dimensional Boltzmann curve, so that the critical buckling stress can be estimated simply and accurately for panels of arbitrary dimensions. A proposed extension of the numerical predictions to combined loading cases has been outlined.

The proposed methods for predicting critical buckling stress are expected to be of value in the aerospace industry, where design curves and other simple heuristic methods continue to be used in the initial design stage because they provide quick solutions without the need for extensive data preparation.

References

[1] Engineering Sciences Data Unit. *Flat panels in shear. Buckling of Long Panels with Transverse Stiffeners.* ESDU 02.03.02, 1971.

[2] Featherston CA, Kennedy D, Weston DJ and Koffi K. Design rules for panel buckling under combined shear, compression and bending. *Proc 4th Int. Conf. on Thin-Walled Structures*, Loughborough, UK, pp 153-160, 2004.

[3] Johnson AE Jr and Buchert KP. *Critical combinations of bending, shear and transverse compressive stresses for buckling of infinitely long flat plates*. NACA Technical Note 2536, 1951.

[4] Gerard G and Becker H, *Handbook of structural stability. Part 1 – buckling of flat plates*. NACA Technical Note 3781, 1957.

[5] Plank RJ and Williams FW. Critical buckling of some stiffened panels in compression, shear and bending. *Aeronautical Quarterly*, Vol. 25, Part 3, pp 165-179, 1974.

[6] Ueda Y, Rashed SMH and Paik JK. Buckling and ultimate strength interaction in plates and stiffened panels under combined inplane biaxial and shearing forces. *Marine Structures*, Vol. 8, No. 1, pp 1-36, 1995.

[7] Kennedy D, Williams FW and Anderson MS. Buckling and vibration analysis of laminated panels using VICONOPT. *ASCE Journal of Aerospace Engineering*, Vol. 7, No. 3, pp 245-262, 1994.

[8] Wittrick WH and Williams FW. Buckling and vibration of anisotropic or isotropic plate assemblies under combined loadings. *International Journal of Mechanical Sciences*, Vol. 16, No. 4, pp 209-239, 1974.

[9] Anderson MS, Williams FW and Wright CJ. Buckling and vibration of any prismatic assembly of shear and compression loaded anisotropic plates with an arbitrary supporting structure. *International Journal of Mechanical Sciences*, Vol. 25, No. 8, pp 585-596, 1983.

[10] Timoshenko SP and Gere JM. *Theory of elastic stability*. 2nd edition, McGraw Hill, 1961.